2021 IEEE 5th Colombian Conference on Automatic Control (CCAC)
October 19-22, 2021. Ibagué, Colombia.

Dynamic model of an aircraft propulsion system with electric motor and propeller

Manuela Montoya Rivera
Facultad de Ingeniería Aeronáutica
Universidad Pontificia Bolivariana
Medellín, Colombia
manuela.montoyar@upb.edu.co

Luis Benigno Gutiérrez
Facultad de Ingeniería Aeronáutica
Universidad Pontificia Bolivariana
Medellín, Colombia
luis.gutierrez@upb.edu.co

***Abstract*—This paper presents a mathematical model for the dynamic behavior of a electric propulsion system for an aircraft. The system is composed of a Li-Po battery, an electronic speed control (ESC), a brushless DC motor (BLDC), and a propeller. Models are obtained for each component of the system and then they are implemented and integrated for numerical simulation in m language in Octave. The model takes into account the hybrid nature of the system, given that the switching dynamics of the ESC is considered as a discrete event model, while the dynamics of the other components is continuous. The parameters used in the simulation have realistic values associated to the model of a small unmanned aerial vehicle (UAV) propulsion system, but with adecuate parameters it could represent the dynamics of a larger scale electric manned aircraft. Simulation results show a reasonable behavior and further work will be done to estimate the parameters for a real UAV prototype, based on the proposed model.**

***Index Terms*—Aircraft electrical propulsion, Dynamic model, Electric motor, Propeller, Li-Po battery, Electronic Speed Control, Octave.**

I. Introduction

The aeronautical industry has turned its interest in recent years towards the use of energies that are more respectful of the environment, so it is important to delve into electric propulsion systems and the development of tools to describe and detail their behavior. For this reason, this work develops the mathematical model in state space of a propulsion system with a brushless electric motor and a propeller, based on the integration of the behavior model of each of its components. The model was implemented in the Octave m language to simulate the dynamic behavior of the system and verify its correct operation.

II. Electric motors in the aeronautical industry

Research on propulsion systems with electric motors has been growing in recent years because they support recent NASA goals to reduce CO_2 emissions by 50% and NOx emissions by 80%, in addition to reducing the aircraft noise. For this reason, institutes such as NASA's Glenn Research Center have begun research on the benefits and challenges that this new type of propulsion brings, recognizing that it will be implemented in a short time [1]. Furthermore, it should be taken into account that, according to ICAO [2], it is expected that by 2050 the combustion efficiency will improve by 2% per year, which is directly related to the reduction of polluting emissions [3].

Along with these investigations has been the implementation of electric motors in unmanned aerial vehicles, such as NASA's solar impulse vehicle, which is the first aircraft to fly 26 continuous hours without the use of fuel [4]. Industry intentions have now turned to experimenting with the use of this type of propulsion in larger aircraft, in order to have less polluting commercial aviation in the future. In 2017, NASA began development of the X-57 that will have 14 electric motors by modifying a Tecnam P2006T aircraft [5]. In the same year, the US company Wright Electric announced the development of the Wright 1 electric motors, which will power an aircraft with capacity for 186 passengers by 2027 and which they plan to test as part of the EasyJet fleet [6]. Australia-based company MagniX has developed two electric motors for aviation applications, the Magni500 was deployed on May 28, 2020 in a Cessna 208B Grand Caravan that flew for 30 minutes over Washington state [7]. Companies such as Boeing and Airbus are also developing research in conjunction with other companies such as Mitsubishi, Kawasaky, Subaru, Siemens and Rolls-Royce, but initially they focused on hybrid propulsion, which will be seen in the near future [8].

About the mathematical modeling of these systems, advancements are limited to the implementation of hybrid or fully electric powertrains in automobiles [9], [10] which have been developed in a broader way and are generally developed in Matlab/Simulink. It is also possible to find the modeling and simulation of lithium ion batteries [11]. For batteries, this work uses the model developed in [12], which proposes a method that includes all the dynamics of the battery predicting the operating time, current and voltage. This consists of an RC circuit model for batteries of Lithium-Ion and NiMH, which by using the correct

978-1-6654-1883-6/21/$31.00 ©2021 IEEE

operating parameters can be used with Li-Po batteries. In addition, an electrochemical model for Li-Po batteries that assumes isothermal operation identifies factors that limit the performance of cells to optimize their design is presented in [13]. Information on brushless electric motors is also found in the literature, including the development of robust control systems for aerial robotics [14], and the characterization of this type of motors in unmanned aerial vehicles [15]. Also presented are advanced models representing the electronic speed control (ESC) ([16], [17]) that are implemented in Matlab to analyze and monitor the dynamic characteristics of the motor. In [15], a method for evaluating and selecting a brushless motor for an unmanned aerial vehicle is presented, based on a black box model. This type of model is also presented in [18] and [19]. In the first, they compare it with a mathematical model, concluding that both are very good approximations for the study of an electric motor of this type, but the black box model presents a better fit. In the latter, they base the model on the ARX structure and simulate it with Matlab tools. [20] presents a model that is simulated in Matlab/Simulink based on the mathematical model of an electrical circuit. In the literature, electronic speed controllers are generally modeled within the motor model, as in [16]. There, they detail the ESC operation within the system without emphasizing its mathematical modeling [21], [22]. In [23] there is quite detailed information on the aerodynamic modeling of the propellers using the Vortex step model to obtain the aerodynamic loads. This type of model is outside the scope of this work, for this reason a more classical model for the propeller is used in this work, such as [24], [25].

It is important to note that the great current challenge of electric propulsion systems, considering their high efficiency in energy conversion and that they generate zero emissions [26], focuses on the improvement of electric energy storage systems, since they do not yet have the energy density necessary to achieve a range that can compete with modern commercial aircraft [27]. Currently, as indicated in [28], Lithium Sulfide batteries are being developed, which can store a greater amount of energy in their cells, in addition, advances have been generated in motors and electronic speed controllers, as shown in [29] but its use and development have been limited by the capacity of current batteries.

Given the need to delve into the subject and develop a complete model that manages to integrate the main components and that serves to continue with the development of this type of systems within the industry, this work is developed generating knowledge that allows the optimization of the electrical aircraft propulsion systems and contribute to the reduction of harmful emissions to the environment.

III. Function, behaviour and model of each components

A. Battery

As indicated in [12] electrochemical batteries are of great importance in electrical systems, since they are capable of converting the chemical energy they store into electrical energy. Battery models capable of predicting current and voltage performance can be used to design circuits, optimize them, and predict its performance with different charge profiles, normally the proposed models are compatible with NiCd, NiMH, Li-ion and Polymer Li-on batteries.

Generally, electrical models are used that use a combination of voltage sources, resistors and capacitors, these models are more intuitive and easy to understand. It is usually possible to classify them into 3 categories: Thevenin, impedance and time-based.

In [12] they have developed a model closer to the real behavior of batteries. This consists of two separate circuits, related to each other by a voltage-controlled voltage source and a current-controlled current source. It has on the left a capacitor that models the state of charge of the battery, a resistance of self-discharge and a current controlled-current source modeling how the the stored charge increases or decreases during the charging and discharging cycles (see Figure 1). On the right side, the internal resistance of the battery and the transient behavior under different loads are modeled using two parallel RC networks in series, modeling the internal impedance of the Thévenin equivalent circuit to represent the transient response. A nonlinear voltage source controlled by voltage represents the open circuit voltage of the battery in terms of the state of charge. The model predicts the battery response in steady state and in the transients, taking into account the electrodynamic characteristics of the batteries (usable capacity, open circuit voltage and the transient response).

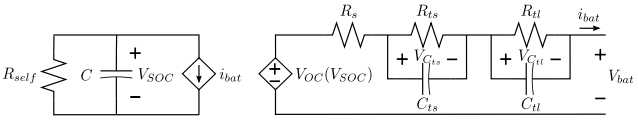

Figure 1: Equivalent electric circuit for battery model

B. Electronic Speed Controller (ESC) and electric motor

Brushless direct current motors (BLDC) are electrically commuted by electronic switches, which replace the use of brushes. These motors, compared to a direct current motor or an induction motor, have higher efficiency, generate less noise, have better dynamic response, they are smaller and lighter and have a higher speed range. In general, this motor converts electrical energy into mechanical energy using electromagnetic principles [30].

The model presented in this work is based on [16], [17]. The set of the brushless direct current (BLDC) motor with

its ESC is composed of three parts: Power conversion with PWM inverters, BLDC motor and its load, and speed and torque controllers, as seen in the Figure 2.

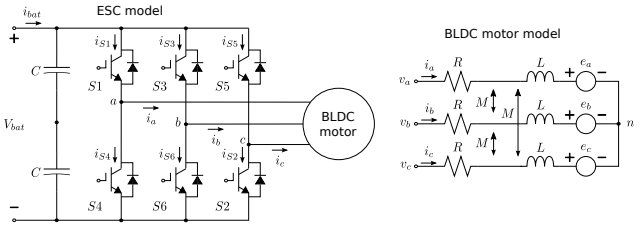

Figure 2: ESC and BLDC motor

The first part of Figure 2 shows the inverter topology, which consists of 6 electronic switches based on IGBTs (Insulated Gate Bipolar Transistors) with a direct current source. The following simplifications are assumed for the engine model:

- Unsaturated motor
- The resistance of all the stator windings is equal and their inductances are constant and equal.
- Power transistors and diodes in the inverter behave as ideal switches.
- Iron losses are negligible, although they are finally included in the model through an efficiency factor.

C. Propeller

1) Classic analysis of control volume - Moment theory: In [24] the propeller model based on the moment theory is presented. In this theory the propeller is approximated as a thin, infinite disk actuator through which the static pressure increases discontinuously, it is based on the following assumptions:

- The speed is constant on the disc.
- The pressure is uniform on the disc.
- The rotation that the flow acquires as it passes through the propeller is neglected.
- The flow passing through the propeller can be separated from the rest of the flow by correctly defining a stream-tube.
- The flow is incompressible

2) Moment theory - Blade element: In [25] a model based on the moment and blade element theory is presented. For the analysis, the pitch angle (β) is defined, which is measured from the blade's zero lift line, pitch is defined in terms of the distance that a propeller can move forward without sliding in one revolution. From this, the contribution of a blade element to thrust and torque is calculated to finally express it in terms of coefficients.

IV. Development of mathematical model in state space of each component

A. Battery

The state space model for a Li-Po battery obtained from Figure 1 is given by the following equations:

$$\frac{dV_{SOC}}{dt} = -\frac{1}{C}\left(\frac{V_{SOC}}{R_{self}} + i_{bat}\right), \tag{1}$$

$$\frac{dV_{C_{ts}}}{dt} = \frac{1}{C_{ts}}\left(i_{bat} - \frac{V_{C_{ts}}}{R_{ts}}\right), \tag{2}$$

$$\frac{dV_{C_{tl}}}{dt} = \frac{1}{C_{tl}}\left(i_{bat} - \frac{V_{C_{tl}}}{R_{tl}}\right), \tag{3}$$

$$V_{bat} = V_{OC}(V_{SOC}) - i_{bat}R_s - V_{C_{ts}} - V_{C_{tl}}, \tag{4}$$

where V_{SOC} represents the voltage across capacitor C, whose stored charge models the stored charge in the battery; R_{self} is the resistance that models the self discharge of the battery (Ω);i$_{bat}$ is the battery current (A); $V_{OC}(V_{SOC})$ is a nonlinear function that models the discharge curve of the battery, the open circuit voltage V_{OC} as a function of V_{SOC} (V); R_s is the internal resistance of the battery (Ω);V$_{C_{ts}}$ is the voltage across the parallel of C_{ts} and R_{ts} modeling short time current transients (V); $V_{C_{tl}}$ is the voltage across the parallel of C_{tl} and R_{tl} modeling long time current transients (V).

B. Electronic motor controller (ESC) and electric motor

According with [16] and [17], the switching logic for the current is defined by the operation of the ESC, taking into account that the ESC is attached to the motor which has 3 terminals and each one has: resistive effect, induced counter electromotive force and inductive effect.
So, an state space model for the BLDC motor with the propeller load added is:

$$\frac{di_a}{dt} = \frac{1}{(L-M)}(v_a - Ri_a - e_a), \tag{5}$$

$$\frac{di_b}{dt} = \frac{1}{(L-M)}(v_b - Ri_b - e_b), \tag{6}$$

$$\frac{di_c}{dt} = \frac{1}{(L-M)}(v_c - Ri_c - e_c), \tag{7}$$

$$\frac{dw}{dt} = \frac{1}{(J_{motor} + J_{prop})}(T_e - T_{prop} - Bw), \tag{8}$$

$$\frac{d\theta}{dt} = w, \tag{9}$$

where i_a, i_b, i_c, are the currents (A) and v_a, v_b, v_c are the voltages in the motor terminals (V); e_a, e_b, e_c are the counter-electromotive forces induced in each motor phase (V); R is the resistance (Ω), L is the inductance associated

with each motor terminal and M is the mutual inductance between terminals (H); T_{prop} is the propeller torque (Nm); J_{motor} and J_{prop} are the moments of inertia of the motor and the propeller (kgm^2); ω is the angular velocity of the motor (rad/s) and θ is the angle of the motor axis (rad).

The electromagnetic torque produced by the motor calculated from

$$T_e = \begin{cases} \eta * K_e * \dfrac{|i_a| + |i_b| + |i_c|}{2}, & w = 0 \\ \eta * \dfrac{i_a * e_a + i_b * e_b + i_c * e_c}{w}, & w > 0 \end{cases} \quad (10)$$

The first case in 10 in included to take into account the initial torque producced by the electromagnetic interaction due to the motor current. Once the motor starts moving the second condition is applied. In this equation η represents the motor efficiency.

This continuous dynamics is accompanied by the discrete event dynamics of the ESC switching of the IGBT bridge. In this work, the PWM logic is modeled in conjunction with the ESC's internal current control loop. The external speed control loop is not included, it will be considered in future work. This discrete dynamics is implemented in a function, the logic used in this function is explained below.

What the ESC does is to switch the electronic switches S1 to S6 of the IGBT bridge so that only two terminals of the motor are connected to the battery voltage for a while, the other terminal is kept open in this period. The function that models the ESC represents the behavior of that switching assuming that the IGBTs and diodes act as ideal switches. The cycles are defined by a variable $ESC_{cycle,k}$, which has values of 1,2,...,6 and then returns to 1,2,...,6 and so on. This variable is set according to the electrical angle of the motor, changing every sixth of an electrical turn. The electrical angle is p/2 times the geometric angle on the motor shaft, where p is the number of magnetic poles of the motor (for the motor considered in this model, p = 14). For example, for cycle 1, $v_{bc} = v_b - v_c = -V_{bat}$. Within each cycle, the current is controlled with a hysteresis cycle, so the current magnitude remains between $0.9i_{max}$ and $1.1i_{max}$. This practically generates a PWM control of the motor current. When ESC switches to cycle 2, $v_{ab} = v_a - v_b = V_{bat}$, in cycle 3 $v_{ca} = v_c - v_a = -V_{bat}$, in cycle 4 $v_{bc} = v_b - v_c = V_{bat}$, in cycle 5 $v_{ab} = v_a - v_b = -V_{bat}$, and finally, in cycle 6 $v_{ca} = v_c - v_a = V_{bat}$. The end result is that the ESC generates an approximate three-phase sinusoidal signal applied to the motor terminals, controlling the maximum current in each cycle.

When the simulations is run, in the model of the BLDC motor only two of the equations 5, 6, 7, are implemented in each cycle, and the current of the other terminal that is open is set to zero. Thas why the variable $ESC_{cycle,k}$ is passed to the model of the BLDC motor. In each cycle the voltage of the battery is connected, disconected, conected,... following the logic of the PWM to control the current of the motor. Given the the model considers the switching dynamics in conjuntion with the switching dynamics, it is required to run the simulation with a very small sample period to capture the switching dynamics.

C. Propeller

For the mathematical model of the propeller, the torque equation is:

$$T_{prop} = \frac{4\rho w^2 r_{prop}^5 C_p(w, J)}{\pi^3}, \quad (11)$$

and the propeller thrust is given by

$$Thrust_{prop} = \frac{4\rho w^2 r_{prop}^4 C_t(w, J)}{\pi^2}, \quad (12)$$

where T_{prop} is the propeller torque (Nm), $Thrust_{prop}$ is the propeller thrust (N), w is the propeller angular velocity (rad/s), r_{prop} is the propeller radius (m), C_p is the propeller power coefficient, C_t is the propeller thrust coefficient. Both, C_p and C_t are dimensionless functions of the propeller angular velocity, w, and the advance ratio, J, which is defined by (12). In (12), V is the aircraft airspeed (axial velocity of propeller respect to air).

$$J = \frac{\pi V}{w r_{prop}}. \quad (13)$$

The functions for $C_p(w, J)$ and $C_t(w, J)$ are calculated from a lookup table previously obtained based on the moment theory cobined with blade element theory [25].

V. Implementation of mathematical model

The figure 3 presents the block diagram that outlines the implementation of the mathematical model in state space for a propulsion system with brushless electric motor and propeller.

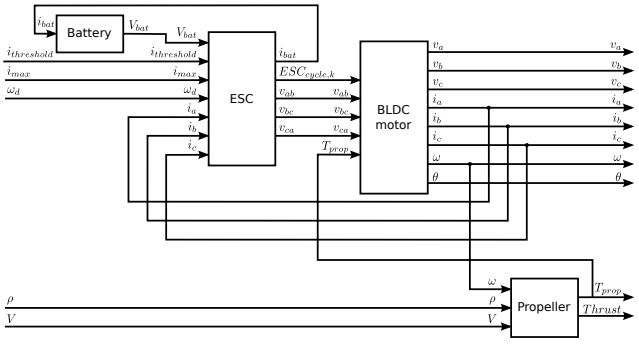

Figure 3: Electric propulsion system block diagram

The model was implemented in Octave's m language. The numerical integration method used to solve the state equations of the state space model was trapezoidal integration

with a sample time close to 1 μs. The discrete event dynamics of the ESC is evaluated prior to each continuous dynamics integration step.

VI. Results

Figures 4, 5, 6 and 7 show the results for a simulation of the electric propulsion system for a time lapse of 10 ms, with a sample time of 0.71429 μs. The simulation shows a short time in order to focus on the details of the ESC switching dynamics.

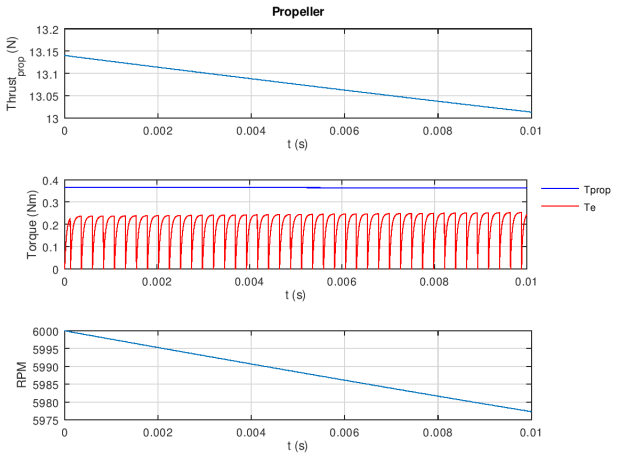

Figure 4: Propeller thrust, torque and RPM

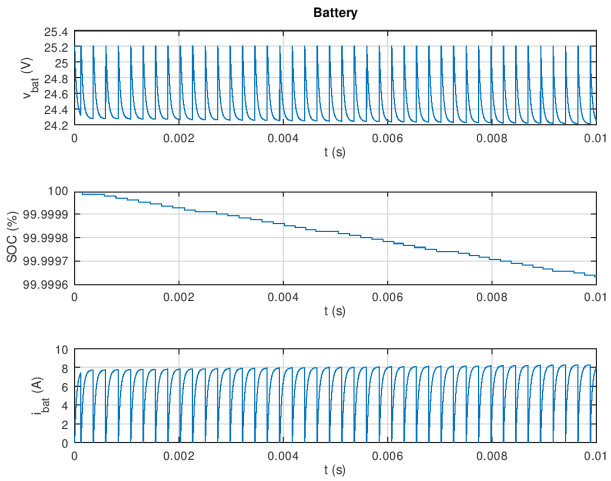

Figure 5: Battery voltage, state of charge (SOC) and current

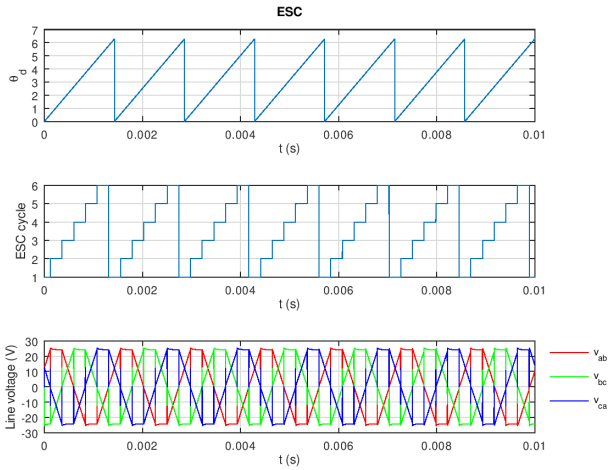

Figure 6: ESC electrical angle, ESC cycle and motor line voltages

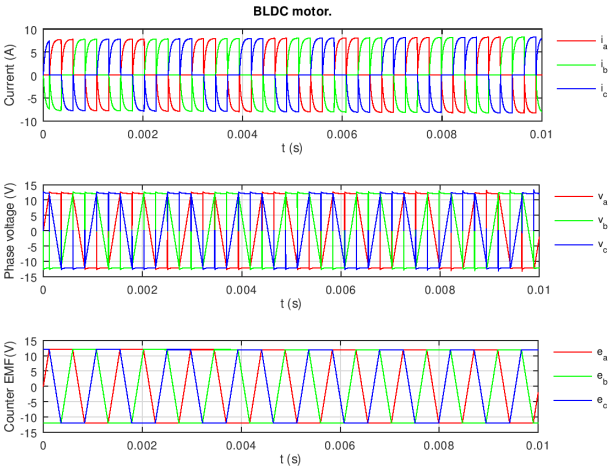

Figure 7: BLDC currents, voltages, Counter-electromotive force

For this case, in figure 4 the thrust and the RPM of the propeller are decreasing, given that the propeller torque is greater than the torque produced by the BLDC motor for the initial RPM value selected for this simulation (6000 RPM).

In Figure 5 the middle graph shows how the battery discharges over time, the other two graphs show the voltage and current of the battery operating with a commutation according to the logic of the ESC and is it is evident that when there is a current peak the voltage is reduced, which shows a behavior in accordance with the real phenomenon. The first graph of figure 6 shows the electrical angle of rotation of the ESC as a function of time. It is confirmed that the electrical angle is equal to seven times the angle of mechanical rotation given that the simulated motor has 14 poles. In the second graph it is confirmed that in each turn of the motor the ESC goes through each of its commutation cycles according to the angle of turn, finally the last graph shows the commutation

of the voltage in each of the terminals, confirming as in each moment the ESC is only supplying voltage to the motor between two of the three terminals.

In the Figure 7 the first graphs show the current and voltage of each of the motor terminals. The third graph shows the behavior of the counter electromotive force (EMF) induced in each motor teminal.

In general, the graphs presented previously have a behavior in accordance with what was expected, which shows that this model allows to know in detail the behavior of an electric propulsion system with a brushless motor and propeller.

VII. Conclusions

A dynamic model of the behavior of a propulsion system composed of a LiPo battery, a brushless electric motor that includes its electronic speed control, and a propeller was developed. The model details the switching logic in the ESC, modeling the IGBTs and diodes as ideal switches, also modeling the discrete event dynamics combined with the continuous dynamics of the BLDC motor and propeller. This makes the simulation to consider the hybrid nature of the dynamics of the system. The simulation of the obtained model was carried out using m language in Octave.

The results obtained in the simulation are realistic according to the common behavior of this type of components, although the values of the parameters used in the simulation are close to the behavior of the propulsion system of a small electric UAV.

Future works that can be carried out based on this model are: the design and simulation of the control system for the entire propulsion system, the acceleration of the simulation using with the implementation in C language based on Octave OCT files, and the system identification based on experimental data using this model and optimization techniques.

References

[1] T. J. Wickenheiser, A. K. Sehra, G. T. Seng, J. E. Freeh, and J. J. Berton, "Emissionless aircraft: Requirements and challenges," *AIAA\ICAS International Air and Space Symposium and Exposition: The Next 100 Years*, no. X, pp. 1–10, 2003.

[2] ICAO, "ICAO 2019 Environment Report," *2019 Aviation and the Environment Report*, vol. 43, no. 3, pp. 21–22, 2019.

[3] A. S. Gohardani, G. Doulgeris, and R. Singh, "Challenges of future aircraft propulsion: A review of distributed propulsion technology and its potential application for the all electric commercial aircraft," *Progress in Aerospace Sciences*, vol. 47, no. 5, pp. 369–391, 2011. [Online]. Available: http://dx.doi.org/10.1016/j.paerosci.2010.09.001

[4] NASA, "Solar Impulse To Fly Across America." [Online]. Available: https://sservi.nasa.gov/articles/solar-impulse-to-fly-across-america/

[5] ——, "X-57." [Online]. Available: https://www.nasa.gov/specials/X57/x-57.html

[6] Wright, "Wright blog." [Online]. Available: https://weflywright.com/updates/

[7] Magnix, "Largest commercial all electric passenger aircraft takes to the skies." [Online]. Available: https://www.magnix.aero/news/

[8] AIRBUS S.A.S, "E-Fan X." [Online]. Available: https://www.airbus.com/innovation/future-technology/electric-flight/e-fan-x.html

[9] S. Zoroofi, "Modeling and Simulation of Vehicular Power Systems," *CHALMERS*, 2008.

[10] G. Eirea, F. Chiaramello, F. Souza, and S. Negrın, "Simulacion de un Sistema de Propulsion Eléctrico para EV," *Iie.Fing.Edu.Uy*, pp. 1–4, 2012. [Online]. Available: https://iie.fing.edu.uy/ geirea/pub/tdla2012.pdf

[11] M. M. R. Iglesias, A. Lago, A. Noguerias, C. Martínez-Peñalver, J. Marcos, C. Quitans and M. Valdés, "Modelado y simulación de una batería de Ion-Litio comercial multicelda." no. November 2016, pp. 464–469, 2015.

[12] M. Chen and G. A. Rincón-Mora, "Accurate electrical battery model capable of predicting runtime and I-V performance," *IEEE Transactions on Energy Conversion*, vol. 21, no. 2, pp. 504–511, 2006.

[13] D. W. Dees, V. S. Battaglia, and A. Bélanger, "Electrochemical modeling of lithium polymer batteries," *Journal of Power Sources*, vol. 110, no. 1, pp. 310–320, 2002.

[14] J. M. Cotte Corredor and A. F. Moreno Pineda, "Diseño de control robusto de velocidad de motores brushless para robótica aérea," p. 100, 2010. [Online]. Available: http://www.bdigital.unal.edu.co/1896/

[15] I. Zhao and Y. Yu, "Brushless DC Motor Fundamentals Application Note," *MPS*, 2011. [Online]. Available: https://www.monolithicpower.com/pub/media/document/Brushless_DC_Motor_Fundamentals.pdf

[16] B. K. Lee and M. Ehsani, "Advanced simulation model for brushless DC motor drives," *Electric Power Components and Systems*, vol. 31, no. 9, pp. 841–868, 2003.

[17] P. Pillay and R. Krishnan, "Modeling, Simulation, and Analysis of Permanent-Magnet Motor Drives, Part ll: The Brushless DC Motor Drive," *IEEE TRANSACTIONS ON INDUSTRY APPLICATIONS*, vol. 25, no. 2, p. 6, 1989.

[18] J. A. Becerra-Vargas, F. E. Moreno-García, J. J. Quiroz-Omaña, and D. Bautista-Arias, "Estimación de parámetros y modelo de caja negra de un motor CD sin escobillas," *TecnoLógicas*, vol. 17, no. 33, p. 55, 2014.

[19] M. S. Hussin, M. N. Azuwir, and Y. N. Zaiazmin, "Modeling and validation of brushless DC motor," *2011 4th International Conference on Modeling, Simulation and Applied Optimization, ICMSAO 2011*, pp. 0–3, 2011.

[20] G. Prasad, N. S. Ramya, P. V. N. Prasad, and G. T. R. Das, "Modelling and Simulation Analysis of the Brushless DC Motor by using MATLAB," *Ijitee*, vol. 1, no. 5, pp. 27–31, 2012.

[21] H. Gónzalez, M. Suell, M. Morales, and O. Lengerke, "DISEÑO MECATRÓNICO DE UN CONTROLADOR DE VELOCIDAD IMPLEMENTADO EN UN ROBOT MÓVIL DE TRACCIÓN SÍNCRONA," *8º Congreso Iberoamericano De Ingenieria Mecanica*, no. 18, p. 9, 2007.

[22] A. Castillo Rueda, "Diseño y fabricación de un longboard eléctrico," 2018.

[23] J. P. Barnes, "Math modeling of propeller geometry and aerodynamics," *SAE Technical Papers*, no. 724, 1999.

[24] P. M. Sforza, "Propellers," in *Theory of Aerospace Propulsion*, 2017, pp. 487–524.

[25] B. McCormick, *Aerodynamics, Aeronautics and Flight Mechanics*, 1994, no. 1.

[26] M. Hepperle, "Electric Flight – Potential and Limitations," *German Aerospace Center*, 2009. [Online]. Available: https://nag.aero/wp-content/uploads/2018/05/MP-AVT-209-09-Electric-Flight-Potential-and-Limitations.pdf

[27] D. Thisdell, "The magic number that makes electric flight viable," *FlightGlobal*, 2020. [Online]. Available: https://www.flightglobal.com/business-aviation/the-magic-number-that-makes-electric-flight-viable/140050.article

[28] M. Crittenden, "With Ultralight Lithium-Sulfur Batteries, Electric Airplanes Could Finally Take Off," *IEEE Spectrum*, 2020. [Online]. Available: https://spectrum.ieee.org/aerospace/aviation/with-ultralight-lithiumsulfur-batteries-electric-airplanes-could-finally-take-off

[29] D. Sigler, "H3X – A Motor with High Power Density," *Sustainable Skies*, 2020. [Online]. Available: http://sustainableskies.org/h3x-motor-high-power-density/]

[30] I. Zhao and Y. Yu, "Brushless DC Motor Fundamentals Application Note," *MPS*, 2011. [Online]. Available: https://www.monolithicpower.com/pub/media/document /Brushless_DC_Motor_Fundamentals.pdf